Eur. J. Phys. 13 (1992) 145–151. Printed in the UK

The formation of Ditchev's rings

R K W Haselwimmer†

Cavendish Laboratory, Cambridge, UK

Received 15 October 1991

Abstract. Novel patterns of iron filings (Ditchev's rings) that seem to defy any classical explanation have recently been reported. These patterns appear when magnetic powder is floated on a liquid surface above a magnet pole In this paper we present more detailed observations that reveal the presence of new open ring and lattice structures.

This paper then considers the subtle balance between magnetic and surface tension interactions to explain all the observed effects classically. The close packed lattice structures have been modelled by considering the forces on separated magnetic particles in a divergent external field, whilst the ring behaviour has been associated with the formation of short radial filaments under magnetic attraction. When lying in dipped fields these microfilaments crucially generate capillary dipoles, and it is the interaction of these that is thought to produce both open and Ditchev's ring structures.

Résumé. Des arrangements nouveaux de Limaille de Fer qui paraissent ne pas avoir d'explication rationelle ont été récemment rapportés. Ces arrangements arrivent lorsque la limaille est mis a flot sur une surface liquide au dessus d'un pôle magnétique. Dans cet article nous rapportons des observations plus detailées qui montrent la présence de structures nouvelles en forme d'anneaux et de réseaux.

Nous considerons l'équilibre subtile entre interactions magnetiques et de tension superficielle qui expliquent tous les effets observés. Les arrangements de réseaux serrés ont été modelisés en considérant des forces qui agissent sur une particle isolée dans un champ magnétique divergent, tandis que le comportement en anneau est associé avec la formation de filaments radials courts sous attraction magnétique. Lorsqu'ils sont placés dans un champ magnétique incliné, ces microfilaments genèrent des dipoles capillaires et c'est l'interaction entre celles-ci qui est sullosée génerer les arrangements ouverts et les anneaux de Ditchev.

1. Introduction

The characteristic patterns that iron filings form around magnets have been known for many hundreds of years now. It is clear that as early as 1600 William Gilbert [1] must have known of the effects of magnets on nearby filings. Later, in 1832 it was Michael Faraday [2] who appreciated fully the importance of these patterns as providing evidence for the independent existence of a magnetic field.

Now it seems that no textbook introduction to magnetism is complete without its classic picture of filings surrounding a bar magnet. So one might be so bold as to think that the field, in both senses of the word, was now fully understood. That is, until Ditchev [3] recently reported here the observation of what are entirely counter-intuitive patterns with magnetic powders. The rings that he finds are quite different from the conventionally expected patterns and appear to defy any classical explanation.

This paper, the outcome of a third-year undergraduate physics project, contains more detailed observations of Ditchev's rings as well as newly found structures. It then presents simple classical models for these effects that consider the interplay between magnetic and surface tension forces.

† Presently at Department of Applied Physics, Stanford University, CA, USA.

2. New observed structure

Ditchev's rings can be produced simply by placing the pole of a bar magnet beneath a shallow dish containing water, and then sprinkling a fine magnetic powder gently onto the liquid surface, as shown in figure 1. The best results sometimes require a little perseverance with magnet position and powder type, and for an interesting account of these conditions and the history of the effect, readers are referred to Ditchev's original letter [3]. In Cambridge the best observations have been made with a permanent magnet and soft iron powder kindly provided by him (via A B Pippard).

Interesting detail can be revealed using a simple laboratory microscope (× 10) but, to produce the plates shown here, black and white photographs were taken using a 35 mm SLR with tripod and 1 : 1 lens attachment, and then enlarged to show extra detail. Figure 2 is fairly typical of the observed patterns and is especially revealing as it shows the existence of much rich and interesting structure. We have chosen to divide the behaviour into the three regimes illustrated

0143-0807/92/030145 + 07 $04.50

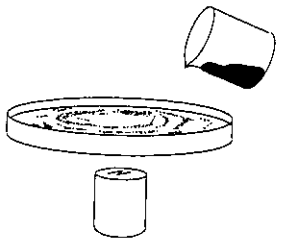

Figure 1. Ditchev's experimental set-up.

in figure 3, which are the central close-packed lattice, a surrounding region of open rings, and an outer band of true Ditchev's rings.

The close-packed lattice may indeed be the only structure observed if very little powder is used. Under the microscope it appears to be composed of single particles separated by about 0.7 mm to form a lattice structure. If the size of these particles is fairly uniform the packing appears to be close to hexagonal in nature (see figure 3(*a*)). As a sidenote it is interesting to note that this type of behaviour is very similar to the packing of flux lines in the mixed state of a type-II superconductor, which can also be visualized using magnetic powders [4].

The open ring region is highly interesting, showing structural similarities to both the close-packing lattice and Ditchev ring regions. As shown in figure 3(*b*), this

Figure 2. Showing the overall powder pattern.

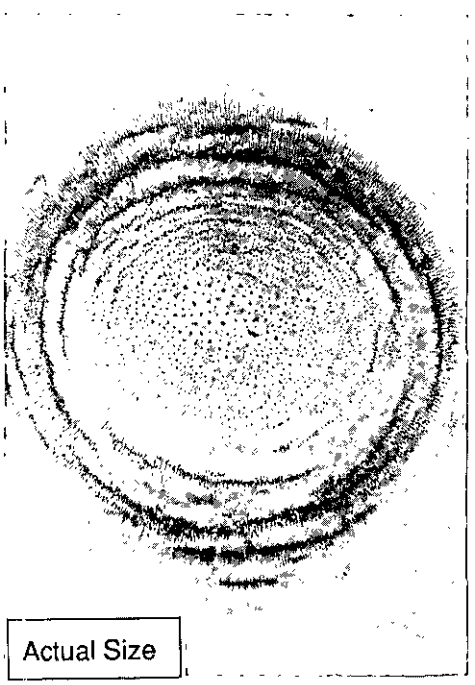

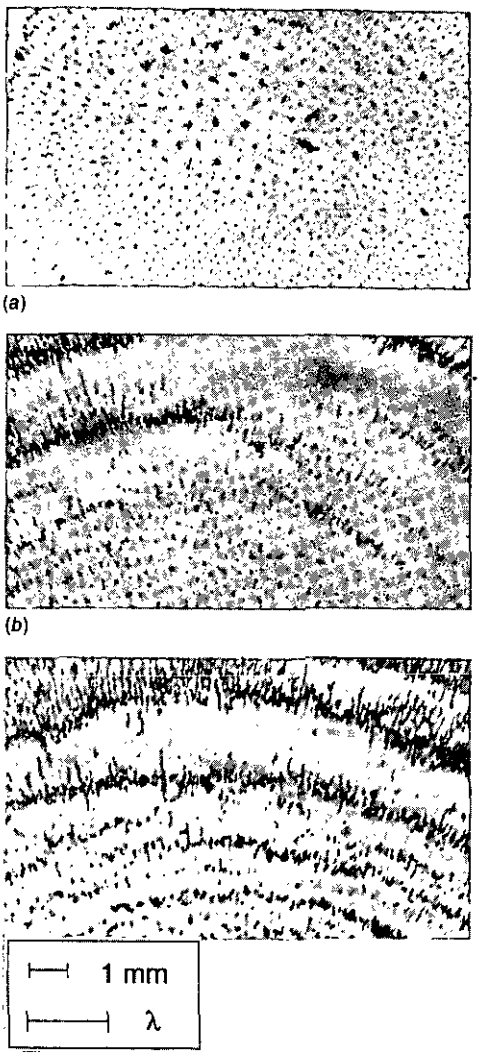

Figure 3. Showing (*a*) the close-packed lattice, (*b*) the open ring and (*c*) the Ditchev's ring regions respectively.

(and, as we shall see, also the Ditchev ring behaviour) is characterized by the presence of short, radially oriented, *microfilaments*. These microfilaments do not seem to be present in the original powder but instead form as small particles join together in the magnetic field. The microfilaments then arrange themselves into loose bands at right angles to the direction of the magnetic field producing an open ring.

Ditchev's rings then form the natural conclusion to the open rings described above. The microfilaments remain oriented radially, but now are in intimate contact, producing the solid rings or arcs first observed by Ditchev and shown in figure 3(*c*).

3. Relevant physics

This system is indeed a complex one—not only must we consider the magnetic particle–particle forces that give rise to conventional patterns, but also particle–magnet forces. The liquid surface also introduces extra, and as we shall see, crucial, effects, through the mutual capillary attraction and repulsion between particles lying on it.

The magnet supplied by Ditchev was fairly short and fat, and field plotting experiments have indicated that it may be modelled as a dipole source for a magnet to liquid surface distance of 3.7 cm. The effective dipole strength was in turn estimated as 6.3 A m^2 by measuring the height from which the magnet would pick up iron powder. Applying the normal dipole formulae produces a field strength at the water surface of the order of 25 mT.

An estimate of the particle size made under the microscope gave an average volume of approximately 1×10^{-13} m^3 and we have ignored any effects due to the shape of particles by treating all as strictly spherical. This makes the analysis of magnetic interactions relatively simple, as spherical magnetized particles generate purely dipole fields (though the geometry of dipole–dipole interactions is not at all trivial it is at least tractable!). Then as a result of the demagnetising effect of their shape, particles are not magnetized to saturation. Thus for spherical particles, the internal field is $(\boldsymbol{B} - \frac{1}{3}\mu_0\boldsymbol{M})$ when an external field $\boldsymbol{B}$ is applied and a magnetization of $\boldsymbol{M}$ per unit volume is induced in the particle. For materials of high susceptibility, such as iron, this internal field almost vanishes, producing a magnetic moment for a particle of volume v that varies linearly as:

$$\boldsymbol{m}_{\text{part}} = 3v\boldsymbol{B}/\mu_0. \tag{1}$$

This effective susceptibility remains valid as long as $\boldsymbol{M}$ is much smaller than the saturation magnetization, $\boldsymbol{M}_{\text{sat}}$, which for iron is 1.7×10^6 A m^{-1}. This implies that $\boldsymbol{B}$ be less than 0.7 T, which is easily satisfied at the water surface.

3.1. Particle–magnet magnetic interactions

Since the external magnet acts as a dipole source, the field above its pole dips away from the vertical as one moves away from the magnet (and pattern) axis. This has the effect of drawing particles rapidly into the pattern centre as well as squeezing together the particles already residing there. This squeezing force is important to the formation of the close-packed lattice. It may be estimated by considering two particles each lying on the liquid surface, a distance x from the magnet axis, as shown in figure 4.

The force on a magnetic dipole lying in an inhomogeneous field is given by $(\boldsymbol{m}_{\text{part}} \cdot \nabla)\boldsymbol{B}$, which becomes

$$\boldsymbol{F} = \frac{3v(\boldsymbol{B} \cdot \nabla)\boldsymbol{B}}{\mu_0}$$

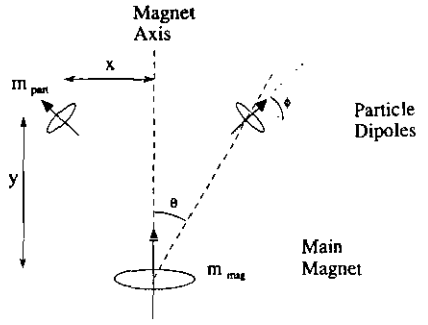

Figure 4. The particle and magnet configuration used in the squeezing calculation.

from (1), because $\boldsymbol{m}_{\text{part}}$ always aligns itself with $\boldsymbol{B}$. By then expanding the Cartesian components of this field in terms of $B_0(y)$, the vertical field strength on the magnet axis, we get:

$$B_x(x, y) = B_0(y)(3x/2y + \dots)$$

$$B_y(x, y) = B_0(y)(1 - 3x^2/y + \dots).$$

From this it follows that the horizontal attractive squeezing force on a particle lying at (x, y) is

$$F_{\text{sqz}} = \frac{3v}{\mu_0}\left(B_x\frac{\partial B_x}{\partial x} + B_y\frac{\partial B_x}{\partial y}\right)$$

$$\Rightarrow F_{\text{sqz}} = \frac{45vB_0^2(y)x}{4\mu_0 y^2}. \tag{2}$$

3.2. Interparticle magnetic interactions

The induced magnetic dipoles described above also interact with one another to produce local structures. Unfortunately, the directionality of this dipole–dipole interaction is not at all trivial and depends on the orientations of the dipoles with respect to the line joining them. In general two dipoles lying in a plane, with parallel magnetizations lying at angle ϕ to the plane, will experience a mutual attractive force:

$$F_{\text{dip}} = \frac{3\mu_0 m_1 m_2(3\cos 2\phi + 1)}{8\pi r^4}. \tag{3}$$

Near the magnet axis ϕ is almost 90° and the force is repulsive, but away from the axis the field dips away from the vertical and when $\phi < 55°$ particles will start to attract one another. It is possible that at angles greater than 55° particles may be induced to join end-to-end, but certainly when $\phi < 55°$ they will start to form filaments which will stand up on the water surface as they align with $\boldsymbol{B}$. It is the form of $F_{\text{dip}}(\phi)$ which gives rise to the two very different types of lattice and ring structure.

3.3. Interparticle capillary interactions

Water is less dense than iron and so can only support iron particles as a result of surface tension forces. So in order to provide an upward component of force, the water surface curves downwards in the region of the particle and, as the particle's weight (or effective weight as a result of magnetic forces) increases, so does this curvature.

It is then easy to see that there will exist a net attraction between particles that both curve the surface downwards, as each particle tries to fall into the hole created by the other. More generally, and as was interestingly also observed by Gilbert [1], two particles that are wetted by the surface in the same sense (i.e. either both depress or both raise the liquid surface) will attract one another, while nearby particles that are wetted in opposite senses will experience a net repulsive effect [5].

By considering how the angle of the liquid surface drops off the distance, we can derive a simple $1/r$ force law for attraction or repulsion between particles (this allows us to draw a direct analogy with two-dimensional electrostatics which also has a $1/r$ force law, except that with capillary effects it is like wettings that attract, while unlike repel)

$$F_{\text{cap}} = -\frac{w_1 w_2}{2\pi T}\left(\frac{1}{r}\right) \tag{4}$$

where w is the weight, or effective weight, of each particle, and T is the surface tension, which for water is $7 \times 10^{-2}\,\text{N m}^{-1}$

There is an extra effect from the liquid which exerts an upward pressure on the surface if it is depressed, or downward if it is elevated. This tends to make the liquid surface curve more sharply than it otherwise would, giving rise to a screening-type force law that drops off as $r^{-1}e^{-r/\lambda}$. (The difference between sleeping on a water-bed and sleeping on a drumskin). The liquid can then be treated as lying at its equilibrium level outside of the screening length, λ, which for a liquid of density ρ and surface tension T is defined as:

$$\lambda = \sqrt{\frac{T}{\rho g}}. \tag{5}$$

In the case of water this gives a length of about 2.5 mm, which is much larger than any of the particle–particle spacings that are observed. (See the scales on plates.) This condition allows us to ignore liquid screening when considering interparticle capillary forces and to use the simpler $1/r$ force law.

4. The close-packed lattice

This behaviour is the simplest to understand qualitatively, as individual particles remain separated and do not form microfilaments. This is because close packing occurs in the centre of the pattern where the field is most nearly vertical and consequently the particle–particle magnetic forces are all repulsive. At the same time the external dipole field acts to squeeze particles together into the pattern core.

Since the magnetic squeezing falls off more slowly than the repulsive interparticle force, particles may sit in equilibrium separated from one another. By considering the balance between the squeezing force and magnetic dipole–dipole repulsion, for two particles of dipole strength m_{part} lying above a magnet of dipole strength m_{mag} (as in figure 4) we can gain an estimate of $2x_{\text{eq}}$, the equilibrium interparticle spacing.

Equation (2) gives the form of the squeezing force F_{sqz}:

$$F_{\text{sqz}} = \frac{45vB_0^2(y)x}{4\mu_0 y^2}. \tag{6}$$

For parallel magnetic dipoles, sitting side-by-side, (3) gives a repulsive magnetic interaction of

$$F_{\text{dip}} = \frac{3\mu_0 m_{\text{part}}^2}{4\pi(2x)^4}$$

which becomes from (1)

$$F_{\text{dip}} = \frac{27B_0^2(y)v^2}{64\pi\mu_0 x^4}. \tag{7}$$

At the equilibrium separation, $2x_{\text{eq}}$, these forces will be equal, and this condition gives the relation:

$$(2x_{\text{eq}})^5 = \frac{6vy^2}{5\pi}. \tag{8}$$

So for a magnet–surface distance, y, of 3.7 cm and average particle size of $1 \times 10^{-13}\,\text{m}^3$ this gives:

$$2x_{\text{eq}} = 0.55\,\text{mm}.$$

It is encouraging that this two-particle calculation yields a spacing similar to that observed experimentally; however it should not be taken too seriously as it neglects the effect of the rest of the lattice surrounding these particles [6]. It is likely that the interparticle spacing depends on these neighbouring particles, but as yet a complete lattice calculation has not been attempted and so it is hard to say just how.

Equation (8) demonstrates how the particle spacing depends, albeit slowly, on the particle size, with larger particles tending to produce larger spaced lattices. Although this effect is weak for the two-particle model, and may in fact also be weak for a perfect lattice, it is easily seen in figure 3(*a*) where large particles or aggregates locally expand the surrounding lattice of smaller particles.

Capillary interactions are not so important at this stage, despite the fact that the magnet exerts a downward force on particles three or four times greater than that due to gravity, and that this accentuates any capillary attractions. Our two typical particles when separated by 0.5 mm will experience a capillary attraction of only $4.4 \times 10^{-12}\,\text{N}$ compared to a squeezing force some twenty times larger at about $1.0 \times 10^{-10}\,\text{N}$.

As we move outwards from the centre of the pattern, the magnetic field starts to dip over from the vertical and it is this that encourages the formation of radial microfilaments to a greater or lesser extent. As we shall see in the following sections it is exactly this that is crucial to the generation of regions of open and Ditchev's rings.

5. Open rings and Ditchev's rings

Previous sections describe how both the open ring and Ditchev's ring regions are populated by short radial microfilaments. These are produced when the external field dips over to such an extent that attractive magnetic inter-particle forces can pull particles together.

We will consider the factors that influence the *length of these microfilaments in the next section*, invoking the concept of and providing experimental evidence of, capillary dipoles. Given this we can then develop an understanding of how microfilaments will arrange themselves with respect to one another, and how ring structures form.

5.1. Microfilament formation

We have already seen from equation (3) that the magnetic inter-particle force varies crucially with the angle of dip of the local magnetic field, and how it becomes attractive only once ϕ has dipped about 35° from the vertical. If this were the only effect that we need consider, as it is with conventional powder patterns, we might then expect an infinite chain of particles to form. However, to explain why these particles form only short microfilaments we need to consider the shape of the liquid surface surrounding these structures.

This may be studied using the technique of near-normal reflection. A light source (a simple 12 V lamp is ideal) is set almost directly above the water surface. Then, by observing from directly overhead, small tilts in the water surface will reveal themselves as extra reflections.

This technique is shown in cross section in figure 5, though an idea of the shape of the whole surface surrounding microfilaments can be gained by moving the light source around the static filament. The configuration shown in figure 5 will produce extra reflections at each end of the microfilament, revealing the parallel tilted surfaces there. Three microfilaments photographed in this configuration are shown in figure 6, with the pattern centre to the right and main reflection to the left of the figure.

This figure shows exactly the extra reflections predicted by figure 5, indicating microfilaments lying tilted up on the water surface at the angle of the local field. Further observations have revealed that the surface surrounding each microfilament is shaped as in figure 7. This tilted microfilament depresses the water surface at one end and pulls it up at the other.

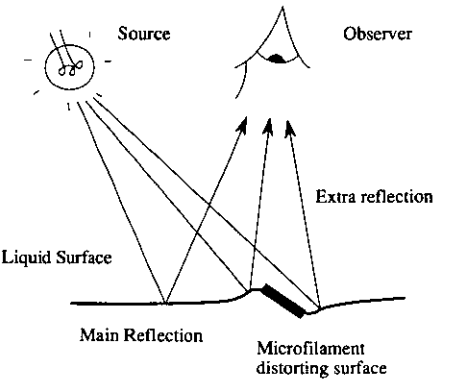

Figure 5. The technique of near-normal illumination to reveal the surface shape (exaggerated).

This corresponds to the creation of what is essentially a *capillary dipole*.

The formation of these capillary dipoles usefully provides us with a mechanism that limits the length of microfilaments. This arises because the magnetic energy gained in producing a microfilament of length L increases only as fast as L, whilst the energy cost in distorting the liquid surface over an area L^2 increases more quickly, as L^2. The result is an equilibrium microfilament length that minimizes the total energy and that depends on the local dip angle of the magnetic field. The shallower the field, the longer the microfilaments are, as shown in figure 8. This produces

Figure 6. Microfilaments observed with near-normal illumination (pattern centre to the right, main reflection to the left).

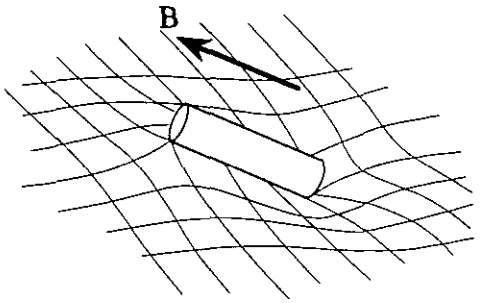

Figure 7. The shape of the liquid surface surrounding a microfilament when tilted up in the magnetic field.

wider microfilament bands near the outer edge of the pattern, which can be seen in figure 2.

The formation of capillary dipoles not only crucially limits microfilament length, but also affects the way in which microfilaments interact with one another. The next section considers the interactions (magnetic and capillary) between microfilaments to show how ring structures form.

5.2. Ring formation

It is now faily easy to see that it is the capillary dipole–dipole interaction that provides all the stability for rings or bands of filaments. For just as oppositely oriented parallel electric dipoles will want to line up side-by-side (with plus to minus and minus to plus), so too will capillary dipoles try to line up side-by-side. So once microfilaments with their associated capillary dipoles have formed they will orient themselves side-by-side and will subsequently form open rings if kept apart by magnetic repulsion, and Ditchev's rings if not.

Rings of capillary dipoles are inherently stable because dipoles lying in a ring will repel dipoles lying in other rings (lying to the inside or outside) and will pull back into the ring any microfilament that might drift out of position in its own ring. In the process this produces banking of the water surface inside, and between rings, which has been observed experimentally using near-normal illumination.

Figure 8. Showing how microfilament length varies with dip angle and with distance from the centre of the pattern.

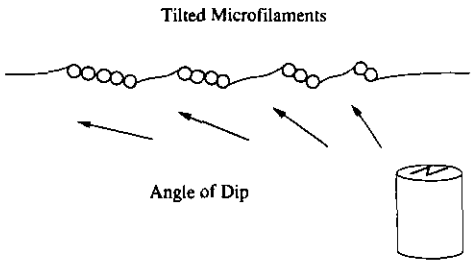

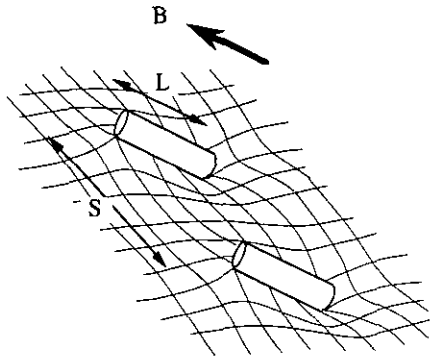

Figure 9. Parallel, tilted microfilaments of length L, and separation S, lying side-by-side on a liquid surface.

To investigate the balance between open and Ditchev ring structures we must consider two parallel, magnetized, capillary dipoles lying side by side as in figure 9. We will deal with microfilaments of length L and separation S and will consider the asymptotic form of the power laws in the two regimes—when $L \ll S$ and when $L \gg S$.

When $L \ll S$, we may use equation (3) to given an S^{-4} dependence in magnetic repulsion and we can derive an S^{-3} variation in the dipole–dipole capillary attraction from equation (4). These two results may be summarized as follows;

$$F_{\mathrm{mag}(L \ll S)} \propto S^{-4} \tag{9}$$

$$F_{\mathrm{cap}(L \ll S)} \propto S^{-3}. \tag{10}$$

In a similar fashion we can evaluate the force laws when the microfilament separation is very much smaller than the microfilament length (i.e. $L \gg S$). In this limit the microfilaments must be treated as thin bar magnets with poles at each end, giving a magnetic pole strength that is independent of L. These magnetic poles can then be treated analogously to electrostatic monopoles (see Hallén [7]) and they consequently experience a repulsive force that varies with distance as S^{-2}. The capillary attraction scales slightly differently, each microfilament being treated as a pair of separated capillary monopoles, yielding a force between each pair that varies like S^{-1}. Summarizing again we produce:

$$F_{\mathrm{mag}(L \gg S)} \propto S^{-2} \tag{11}$$

$$F_{\mathrm{cap}(L \gg S)} \propto S^{-1}. \tag{12}$$

These variations can best be displayed on the log–log force–separation plot shown in figure 10, for a fixed microfilament length, L. This reveals a stable equilibrium separation, S_{eq}, between microfilaments. Should more than two microfilaments be available, these will also sit separated from one another, forming an *open ring*. The equilibrium separation, S_{eq}, importantly varies with microfilament length since the

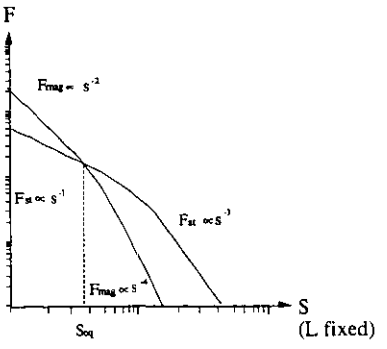

Figure 10. Log–log plot of magnetic and capillary forces against distance for microfilaments of fixed length, lying side-by-side.

magnetic repulsion is independent of L for neighbouring microfilaments, whilst the capillary attraction increases roughly as L^2. As a result, longer microfilaments (at a fixed magnetic dip angle) will lie closer together.

However, it is the dip angle that determines the microfilament length, as the total filament energy (magnetic and capillary) is minimized. Therefore finding the relationship between dip angle and microfilament separation would require a more involved calculation than we can attempt here. Also, non-nearest-neighbour interactions would make the validity of such a two-filament calculation questionable anyway. As a result, it is not easy, and may not even be possible, to state at what field dip angle, open rings, containing separated microfilaments, will turn into Ditchev's rings, containing microfilaments in contact. Indeed, if you study figure 3(*b*) and (*c*) you will find rings where both types of behaviour exist in the same ring structure and at the same field dip angle.

6. Conclusion

We have described the production of Ditchev's original rings, together with new observations of other structures, namely the close packed lattice and open rings. These observations have highlighted the important formation of *radial microfilaments*, which have been found essential in explaining the observed ring structures.

The close packed lattice behaviour has been explained simply with reference to the balance between magnetic dipole–dipole repulsion and the squeezing due to the external field. The inter-particle spacing estimated at 0.55 mm with this model has fortuitously been found to be consistent with the experimentally observed spacing of about 0.7 mm.

The open and Ditchev ring behaviour have both been treated using the same theoretical model. This links ring formation to the formation of radial microfilaments and the generation of capillary dipoles. These microfilaments form due to magnetic particle–particle attraction, while the microfilament length is determined in dipped fields by the balance between magnetic energy gained by lengthening a filament and the energy required to distort the liquid surface over a larger area.

Microfilaments lying in dipped fields twist the liquid surface both up and down forming what is effectively a *capillary dipole*. These surface dipoles, as well as limiting microfilament length, then also act crucially to position microfilaments side-by-side. Should magnetic repulsion, which becomes decreasingly effective as microfilaments lengthen, not be able to keep the filaments apart under their capillary dipole–dipole attraction, Ditchev's rings will form, otherwise open rings will result.

Observations using near-normal illumination have revealed how dipped microfilaments produce these surface dipoles, and how rings of such dipoles repel one another by surface tension.

The models described here appear to give a realistic and consistent explanation of all the observed lattice and ring structures, as well as being very physically meaningful, and it is hoped that further experiments may provide more quantitative tests of these preliminary models.

Acknowledgments

I would like to thank Professor Sir Brian Pippard for first bringing Ditchev's observations to my attention, for correcting my understanding of the close-packed lattice and for supervising the production of this paper. I would also like to thank Dr Robin Ball for supervising the original project and for highlighting the physical importance of asymptotic analysis.

References

[1] Gilbert W 1600 *De Magnete*, (trans P Fleury Mottelay 1893 repr. 1958 (New York: Dover))
[2] Faraday M 1851 *On the Lines of Magnetic force* (*Rl Proc.* (*1851-54*) **1** 105)
[3] Ditchev H 1991 *Eur. J. Phys.* **12** 101
[4] Essman U and Traüble H 1967 *Phys. Lett.* **24A** 526
[5] Poynting H J and Thomson J J 1903 *Properties of Matter* (repr. 1947 (London: Griffin) 188)
[6] Pippard A B 1991 *Private communication*
[7] Hallén E 1962 *Electromagnetic Theory* (London: Chapman & Hall) p 185